Geosciences and Geological and Petroleum Engineering Faculty Research & Creative Works

Geosciences and Geological and Petroleum Engineering

01 Jan 2023

Transport And Plugging Performance Evaluation Of A Novel Re-Crosslinkable Microgel Used For Conformance Control In Mature Oilfields With Super-Permeable Channels

Adel Alotibi

T. Song

Baojun Bai
Missouri University of Science and Technology, baib@mst.edu

Thomas P. Schuman
Missouri University of Science and Technology, tschuman@mst.edu

SPE-215168-MS

Transport and Plugging Performance Evaluation of a Novel Re-Crosslinkable Microgel Used for Conformance Control in Mature Oilfields with Super-Permeable Channels

Adel Alotibi, Kuwait Institute for Scientific Research / Department of Geosciences and Geological and Petroleum Engineering, Missouri University of Science and Technology; T. Song and Baojun Bai, Department of Geosciences and Geological and Petroleum Engineering, Missouri University of Science and Technology; T. P. Schuman, Department of Chemistry, Missouri University of Science and Technology

Abstract

Preformed particle gels (PPG) have been widely applied in oilfields to control excessive water production. However, PPG has limited success in treating opening features because the particles can be flushed readily during post-water flooding. We have developed a novel micro-sized Re-crosslinkable PPG (micro-RPPG) to solve the problem. The microgel can re-crosslink to form a bulk gel, avoiding being washed out easily. This paper evaluates the novel microgels' transport and plugging performance through super-permeable channels. Micro-RPPG was synthesized and evaluated for this study. Its storage moduli after fully swelling are approximately 82 Pa. The microgel characterization, self-healing process, transportation behavior, and plugging performance were investigated. A sandpack model with multi-pressure taps was utilized to assess the microgel dispersions' transport behavior and plugging efficiency. In addition, micro-optical visualization of the gel particles was deployed to study the particle size changes before and after the swelling process. Tube tests showed that micro-RPPG could be dispersed and remain as separate particles in water with a concentration below 8,000 ppm, which is a favorable concentration for gel treatment. However, during the flooding test, the amount of microgel can be entrapped in the sandpack, resulting in a higher microgel concentration (higher than 8,000 ppm), endowing the gel particles with re-crosslinking ability even with excessive water. The microgel could propagate through the sandpack model, and the required pressure gradient mainly depends on the average particle/pore ratio and gel concentration. The gel dispersion significantly reduced channel permeability, providing sufficient resistance to post-water flooding (more than 99.97 % permeability reduction). In addition, the evaluation of micro-RPPG retention revealed that it is primarily affected by both gel concentration particle/pore ratios. We have demonstrated that the novel re-crosslinkable microgel can transport through large channels, but it can provide effective plugging due to its unique re-crosslinking property. However, by this property, the new microgel exhibits enhanced stability and demonstrates resistance to being flushed out in such high-permeability environments. Furthermore, with

the help of novel technology, it is possible to overcome the inherited problems commonly associated with in-situ gel treatments, including chromatographic issues, low-quality control, and shearing degradation.

Introduction

The excessive production of flooding fluids, such as water, polymer solutions, and gas, in mature oilfields due to poor sweep efficiency has led to significant operational costs and, ultimately, the abandonment of wells when the economic viability of production becomes compromised. The primary factors contributing to this issue are the disparity in viscosity between oil and water and the presence of thief zones, particularly high conductivity fractures. These thief zones tend to absorb the injected water, leaving behind a substantial volume of un-swept hydrocarbons within the reservoir (Coste et al., 2000; Yuan et al., 2021). An effective strategy to mitigate the excessive production of injected fluids involves improving the injection profile and modifying the reservoir permeability (Bai et al., 2013). Polymer gel treatments are commonly employed as profile control agents and permeability reducers in such reservoirs (Jin et al., 2014; Gu et al., 2018; Pu et al., 2018; Zhao et al., 2018). It has been successfully used to improve sweep efficiency and mitigate excess water production for a few decades. Different types of gel systems have been developed, such as in-situ gels (Sydansk & Romero-Zeron., 2011), preformed bulk gels (Seright., 1997), partially preformed gels (Sydansk et al., 2004), millimeter-sized preformed particle gel (PPG) (Pyziak & Smith., 2007; Bai et al., 2007a; Larkin & Creel., 2008; Vasquez et al., 2008; Targac et al., 2020), pH-sensitive crosslinked polymers (Huh et al., 2005), and microgels (Chauveteau et al., 2000; Goudarzi et al., 2015). In the oil field, in-situ gel systems are widely recognized as the most employed option compared to other gel types. It is formulated to undergo gelation within the reservoir, triggered by specific conditions such as temperature, pH, or chemical reactions. Although commonly used, in-situ gels have some inherent drawbacks that can limit their effectiveness in specific applications, such as uncontrollable gelation because of the phase separation during transportation and formation damage due to entering oil zones. The development of preformed particle gel (PPG) emerged as a solution to address the limitations associated with traditional in-situ gels. PPG has gained significant attraction in the past decade as a preferred conformance control treatment in many mature oil fields. This is primarily due to its advantageous characteristics, such as low sensitivity to the reservoir environment and the ability to be produced with controlled strength and size at the surface (Bai et al., 2007a). However, current particle gels may not be able to efficiently plug open fractures, fracture-like channels, or conduits, which can limit their effectiveness in certain applications. Field applications have revealed that PPGs may not be highly effective in plugging reservoirs with high water cuts of 85% or more (Qiu et al., 2017). Therefore, a novel re-cross-linkable preformed particle gel (RPPG) has been specifically developed to address the limitations associated with both the in-situ gel and PPG systems. By incorporating re-crosslinking capabilities (self-healing), the B-RPPG offers enhanced performance and versatility compared to its predecessors (Pu et al., 2019; Tao et al., 2022). After being placed in the fractures, the gel particles can re-crosslinking to form a robust rubber-like bulk gel, efficiently sealing the fractures. Factors affecting mechanical strength and stability have been elucidated in previous publications (Pu et al., 2019; Tao et al., 2022).

It should be noted that apart from physical strength and hydrolytic thermal stability, the propagation, retention, and plugging efficiency characteristics also play crucial roles in determining the success of gel treatments. Therefore, comprehending the mechanism behind gel injection and the factors influencing the gel's resistance to water flow through these features are important for achieving a successful conformance control treatment (Imqam et al., 2015). Several studies have been conducted to assess the propagation mechanism of gel systems through high permeability streaks and fractures in oil reservoirs. Seright et al. (1999) conducted a study on HPAM/Cr (III) in-situ gel or HPAM/Cr (III) bulk gel propagation/extrusion through fractures. The experiments involved a variety of fracture lengths and heights, as well as a wide range of gel injections. The study found that the mechanism of gel extrusion through fractures is primarily influenced by three key factors: gel composition, gel volume, and optimum gel placement. Wu and Bai et

al. (2008) developed a numerical model to investigate the propagation of preformed particle gel in porous media. Their study focused on understanding the dynamics of gel flow and transport in porous media and evaluating the factors influencing gel propagation and plugging efficiency. Imqam et al. (2015) studied the plugging performance of preformed particle gel to water flow through large opening void space conduits. Zhao et al. (2021) investigated the transport behavior of swellable microgel particles in super-permeable channels for conformance control. The study was conducted on sandpack with permeabilities ranging from 27 to 221 Darcie to mimic the super-K channels. Multi-taps pressure sensors sandpack model were used to estimate the pressure gradients in different sections of the sandpack. Based on the results, it has been determined that the ratio of particles to pores is a critical factor in the propagation of microgels. As the ratio increases, the pressure required for gel injection also increases. Yuan et al. (2021) carried out an experimental study focusing on the matched particle size and viscoelastic properties of the PPG. The study aimed to find the best-matched particle gel for given reservoirs using a sandpack model. Gourazi et al. (2015) conducted an experimental study on the retention characteristics of PPG in porous media. The study found that PPG retention decreased as the porous media's flow rate, permeability, and temperature increased. Furthermore, in their study (Yao et al., 2020), the researchers delved deeper into the effects of various factors on the transport and retention patterns of the deformable polyacrylamide microspheres. They specifically investigated the impact of flow rate, pore-throat size, particle size, and injection concentration on these patterns. The article identifies five different types of transport and retention patterns, including surface deposition, smooth passing, direct interception, deforming remigration, and rigid.

This study aimed to assess the feasibility of employing micro-RPPG in field applications, such as hydraulic fractures or porous-medium-type channels. To the best of our knowledge, no previous studies have investigated the factors influencing the propagation of novel micro-RPPG. To achieve this, a super-permeability sandpack model was utilized to simulate relevant conditions and investigate factors affecting the transport behavior of micro-RPPG, including concentration, particle/pore ratio, sandpack permeability, and plugging performance.

Experiment

Experimental Material

Re-crosslinking Preformed Particle Gel. The micro-sized branched self-healable preformed particle gel (micro-RPPG) was prepared based on our previous publication (Tao et al., 2022). The RPPG samples were ground and classified into three groups of dry particles using standard U.S. sieves, including 50-100 mesh (297μm - 149μm), 100-170 mesh (149μm - 88μm), and 170-230 mesh (88μm - 54μm).

Brine. In this study, two brines were used for swelling and carrying microgel. The first brine is 2 wt % potassium chloride, and the second brine is synthesized formation water with a total dissolved solid of 57,000 ppm, as shown in Table 1.

Table 1—Brine chemical compositions of formation water.

Composition	Concentration (ppm)
Na^+/K^+	20,043
Ca^{2+}	2,172
Mg^{2+}	658
Cl^-	28,916
HCO_3^-	3,063
SO_4^{2-}	2,977
Total	57,829

Proppant Sand. A quartz sand proppant of 20/30 mesh (Fig. 1) has been used for all experiments provided by Covia™. The relative density and sphericity of the quartz sand are 2.65 and 0.9, respectively.

Figure. 1—(A) Proppant quartz sand of 20/30 mesh and (B) Micro-sized RPPG of 170/230 mesh.

Experimental Setup and Procedure

Swelling and Rheology Behavior of Micro-RPPG. The swelling kinetic behavior was investigated by immersing weighted dry gel particles in the brine until the swelling ratio of micro-RPPG tended to be constant. The swelling ratio was determined as a function of time using Eq. 1.

$$SR = \frac{V_t}{M_i} \tag{1}$$

Where V_t is the volume of swollen microgel at a specific time, and M_i is the weight of dry particles (Pu et al., 2019).

The microgel particle size distribution was examined with an optical microscope (HIROX digital microscope KH-8700). A random sample of 100 fully swelled gel particles was selected, and their sizes were measured according to Feret's diameter method.

The viscoelastic properties of the fully swollen microgel were evaluated using a Haake MARS III rheometer manufactured by Thermo Scientific Inc. The rheological test was performed within the linear viscoelastic region, maintaining a constant frequency of 1 Hz and a strain of 1%.

Sandpack Experimental Procedure. A multi-pressure taps sandpack model (Fig. 2) was utilized as a super-permeable porous media for evaluating the micro-RPPG's transport behavior. The sandpack has a diameter of 25 mm and a length of 500 mm. Four pressure sensors were attached across the model at specific distances to observe the pressure responses at different locations in the sandpack. Two proper mesh sizes were used at both ends of the sandpack to prevent sand production. ISCO syringe pump was used to inject micro-RPPG suspensions and brine from the accumulator to the sandpack tube. The accuracy of the pump is ≤± 1.0%. A high-pressure magnetic stirrer accumulator with a high mixing capacity was used to spread the particle gel within the carrier brine during the injection process. A dry-packing method was applied to pack the quartz sand under continuous shaking. We conducted six experiments examining the effect of particle sizes, concentration, and salinity on the propagation and plugging efficiency, as shown in Table 2. For all the experiments, the temperature was 22°C. A brief description of the experimental procedure is presented below:

1. Sandpack preparation: Firstly, the quartz sand underwent a thorough washing process to eliminate any dust particles. Next, it was dried in an oven for 24 hours. Afterward, the dry sand was tightly packed into the sandpack tube, and the weight of the sand was measured to determine the pore volume and porosity using Eq. 2.

$$PV = V_{SP} - \left(\frac{W_S}{\rho_S}\right), \tag{2}$$

Where PV is pore volume (cm^3), V_{sp} is the bulk volume of the sandpack, W_s is the dry weight of packed sand (gm), and ρ_s is the quartz sand density in (g/cm^3).

2. Initial water injection: The sandpack was vacuumed and saturated with designated brine. Initial water injection was carried out by injecting brine at different flow rates to measure the pressure drops across the sandpack. Then permeability was obtained using Darcy equation Eq. 3. Average pore throat diameter of the sandpack was estimated using the Carman-Kozeny equation (Carman, 1956; Mauran et al., 2001) Eq. 4.

$$Q\mu L = k(A\Delta p), \tag{3}$$

$$d = \sqrt{\frac{16kf_{ck}\tau^2}{\emptyset}}, \tag{4}$$

Where k is the permeability of the sandpack (D), Q is the volumetric flow rate (cc/min), L is the length of the sandpack (cm), μ is the dynamic viscosity (cp), A is the cross-section area (cm^2), and ΔP is total pressure drop (atm), d is the diameter of the pore throat (μm), f_{CK} is the Carman-Kozeny shape factor, τ is the tortuosity, and $\emptyset$ is the porosity.

3. Micro-RPPG injection: A suspension of different micro-RPPG concentrations and particle sizes was injected into the sandpack at a constant flow rate of 3 cc/min, equivalent to Darcy velocity of 28.5 ft/d. The injection process was stopped when a microgel was produced, and a stable pressure drop was achieved. The pressure sensor repones and time was recorded, and the resistance factor (F_r) was calculated using Eq 5. Then the system was shut off for three days, allowing the micro-RPPG to re-crosslink.

$$F_r = \frac{\lambda_w}{\lambda_{gel}} = \frac{\Delta p_{gel}}{\Delta p_{ini-w}}, \tag{5}$$

4. Post-brine injection: After aging the microgel in the sandpack, several PVs of the same brine were injected. The brine breakthrough pressure (the pressure at which the first brine droplet appears in the outlet) and the stable injection pressure for each section were recorded. The residual resistance factor (Frr) and plugging rate (η) established by microgel were calculated using Eq. 6 & 7.

$$F_{rr} = \frac{k/\mu_w}{\lambda_{gel}/\mu_{gel}} = \frac{\Delta p_{gel}}{\Delta p_w}, \tag{6}$$

$$\eta = 1 - \frac{k_{wa}}{k} = 1 - \frac{1}{F_{rr}} \tag{7}$$

Where ΔP_{gel} is the stable injection pressure during microgel dispersion solution injection (psi), ΔP_w is the stable injection pressure during post-brine flooding (psi), μ_w, and μ_{gel} are the viscosity of injection water and microgel dispersion solution, respectively (cp).
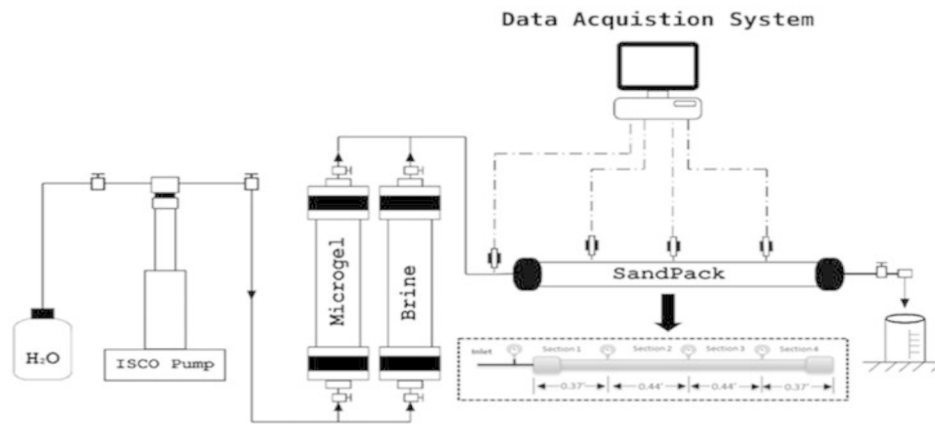
Figure. 2—The simplified schematic diagram of the sandpack model.

Table 2—Summary of sandpack and gel properties for each experiment.

Exp	Porosity (fraction)	K_{ini} (D)	Dry size (μm)	Avg. Swelling size (μm)	Avg. pore size (μm)	Particle/ pore (ratio)	Concentration (ppm)	Brine
1	.33	61	54-88	270	112	2.41	7000	2 wt.% KCl
2	.31	67	54-88	270	118	2.27	5000	2 wt.% KCl
3	.33	59	54-88	270	109	2.47	3000	2 wt.% KCl
4	.30	52	88-149	480	107	4.46	5000	2 wt.% KCl
5	.33	58	88-149	360	112	3.18	5000	*FW
6	.32	58	149-297	685	113	6.05	5000	2 wt.% KCl

*FW: Formation Water

Results and Discussion

Characterization of Micro-RPPG Properties

Swelling Behavior of Micro-RPPG.　　To determine the effect of the particle size on the swelling behavior, dried micro-RPPG with average particle sizes of 75 μm (170-230 mesh), 118 μm (100-170 mesh), and 223 μm (50-100 mesh) were used for the swelling ratio measurement. All the particle size ranges are compared in Fig. 3, which displays the swelling curves for micro-RPPG prepared by 2 wt% KCl and formation water. The measured swelling ratios were found to be independent of particle size. The average equilibrium swelling ratio for the samples prepared by 2 wt% KCl and formation water was found to be 42 and 38 mL/ g, respectively. As anticipated, the swelling rate was faster for the smaller particle gel. It required less than 2 minutes for the 75 μm and 118 μm samples to reach their equilibrium swelling ratio but approximately 2-4 minutes for the 223 μm samples to reach their equilibrium swelling ratio. The results show that the salinity of brine has a significant impact on micro-RPPG swelling kinetics. The particles prepared with 2 wt % KCl demonstrated relatively faster swelling kinetics when compared to particles prepared with formation water. Elevated salinity was found to hinder the swelling rate and decrease the equilibrium swelling ratio. In high-salinity solutions, the polymer chains experienced significant compression, and the electric repulsion between these chains was impeded (Tao et al., 2022).
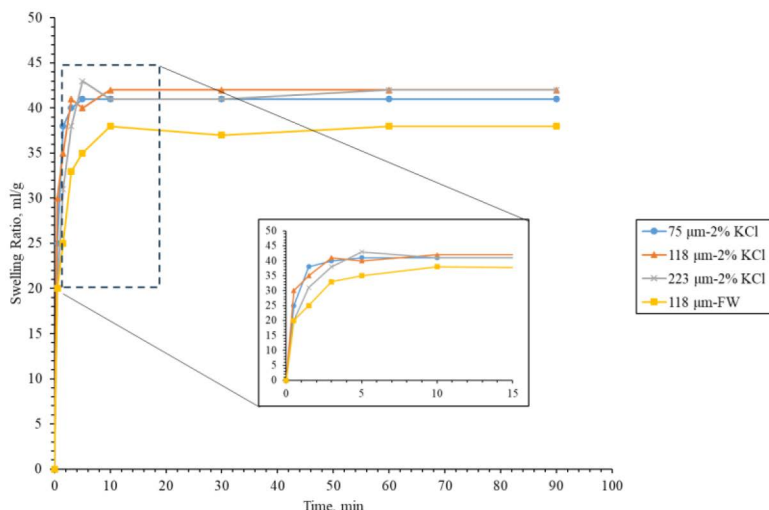
Figure. 3—The swelling kinetics of micro-RPPG in 2% KCl and formation water.

Fig. 4 presents the particle size distribution analysis of each sample after reaching the equilibrium swelling ratio. The results reveal a skewed distribution, indicating variations in the particle sizes within each sample. Notably, it was observed that for some particles, they tended to attach to one another, forming clusters and aggregating into larger particles. This phenomenon can be attributed to the strong aggregation phenomena resulting from the high surface area and energy properties of micro-RPPG.
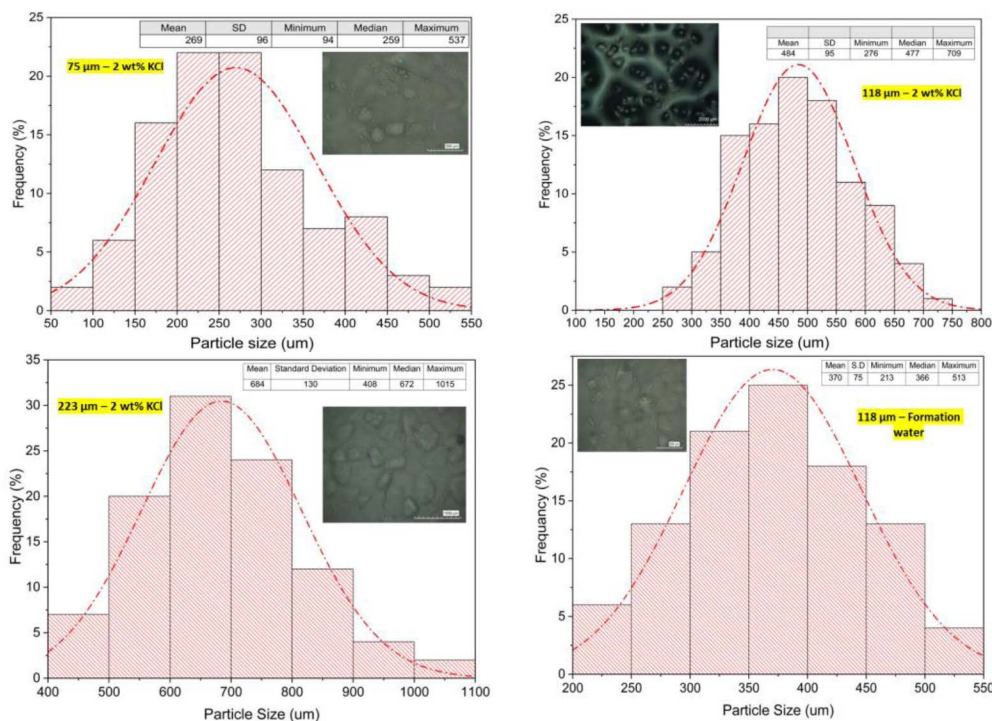

Figure. 4—Particle size distribution of a fully swelled micro-RPPG for different dry particle sizes and brine.

Re-crosslinking Behavior and Gel Strength.   To investigate the re-crosslinking behavior, four different micro-RPPG suspension concentrations, 3000, 5000, 7000, and 8000 ppm, were prepared in 2 wt.% KCl brine. The samples were aged for three days at ambient temperature to reach their maximum swelling size. The results revealed an interesting trend where increasing the concentration activated the re-crosslinking process between particles. Notably, a viscoelastic gel was formed at a concentration of 8000 ppm, while

at 7000 ppm and lower, the microgel was in a suspension form (no re-crosslinking). This finding suggests that the particle gel can promote re-crosslinking interactions among the particles at specific suspension concentrations. Micro-RPPG contains two types of crosslinking agents added during the synthesizing process. The first crosslinking agent entangles the polymer chains to form a permanent 3D network structure, while the second crosslinker agent forms physiochemical bonds among the gel particles interface during the swelling process (Tao et al., 2022). The micro-RPPG's ability to re-crosslink depends on the concentration of the second crosslinker agent present on the outer surface of the swollen gel particle. A fully swelling particle gel has a comparably low second crosslinker agent concentration on the particle's outer surface, resulting in a low tendency to re-crosslink. At low microgel suspension concentration, the particles are suspended in the solution, while at 8000 ppm, there is no free water within the gel, suggesting the particle is partially swelled and therefore has more tendency to re-crosslink and form a bulk gel Fig. 5. The same behavior has been observed in samples prepared in formation water. At concentrations exceeding 8000 ppm, the micro-RPPG can undergo re-crosslinking, resulting in the formation of a highly viscoelastic gel. However, it is worth noting that the re-crosslinking process is considerably slower when compared to samples prepared in a 2 wt% potassium chloride solution.
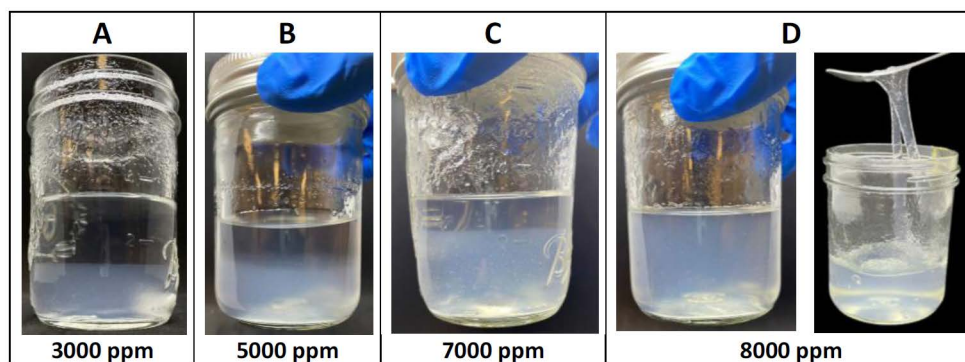

Figure. 5—Pictures A, B, and C are a bottle test of micro-RPPG suspensions with concentrations of 3000, 5000, and 7000 (ppm), respectively. The microgels in the suspension are observed to have settled at the bottom of the beaker, forming separated particles without re-crosslinking. However, when the beaker is stirred, the microgels can be uniformly suspended throughout the solution. In picture D, the microgel concentration is 8000 ppm, exhibiting a highly viscoelastic bulk-gel consistency (re-crosslinked). There is no visible free water suggesting partially swelling particles.

The gel strength was evaluated using the elastic modulus (G'). The tests were conducted within the linear viscoelastic range, using dry particles with an average size of 118 μm and 5000 ppm gel concentration. The results demonstrated that gel strength has an average elastic modulus of 81 pa. In addition, salinity has a negative impact on the gel strength. For example, at the same gel concentration, the gel strength reduced to 66 Pa in formation water.

Transport of Micro-RPPG in Sandpack Model
The transport behavior of the micro-RPPG under different particle/pore ratios, concentrations, and salinity was analyzed according to the pressure curve pattern, resistance factor, micro-RPPG retention, and liquid effluent status. Throughout the injection process, it is assumed that the micro-gel is injected in the form of separate particles without any re-crosslinking process taking place. Contrary to this assumption, the occurrence of re-crosslinking processes cannot be disregarded, particularly due to the observed increase in gel concentration/retention during the injection process in the sandpack.

Gel Injection Pressure Behavior.   Fig. 6 presents the pressure curve at each pressure sensor across the sandpack (Exp 4). In this experiment, a micro-RPPG suspension with a concentration of 5000 (ppm) was injected into a super-permeability sandpack (52 Darcy). The injection rate was set at 3.0 (cc/min). The injection process continued until the particle gel was produced and reached a stable pressure state

at each pressure point. The pore diameter was estimated by using the Carman-Kozeny equation (Eq. 4), and the particle/pore ratio was calculated to be 4.46. During the first four injected pore volumes (PV), the pressure performance of P1 demonstrated an almost linear steep increase. Following that, the pressure curves displayed significant fluctuations, which can be attributed to the higher concentration of microgels accumulating at the forefront of the gel bank, along with the remigration of microgel particles through the narrow pore throats (Zhao et al., 2021). After injecting 7.6 PV, the gel suspensions were produced from the outlet. Likewise, when the gel bank front reached pressure sensor P2 (corresponding to 2.6 PV), the pressure curve exhibited a behavior similar to P1, displaying a steep pressure increase followed by a high fluctuation curve. In contrast to P1 and P2, pressure sensors P3 and P4 demonstrate a gradual and sustained increase in pressure as the gel bank front initially reaches these sensors (4.4 and 6.7 PV, respectively). Once the gel suspension is produced from the outlet, the pressure response observed by all pressure sensors stabilizes, resulting in average stable pressures of 329, 231, 87, and 32 psi for P1, P2, P3, and P4, respectively. This stabilization in pressure is a result of the micro-RPPG attaining stable retention within the sandpack, demonstrating a good capability of micro-RPPG to continuously deform and migrate within the model.
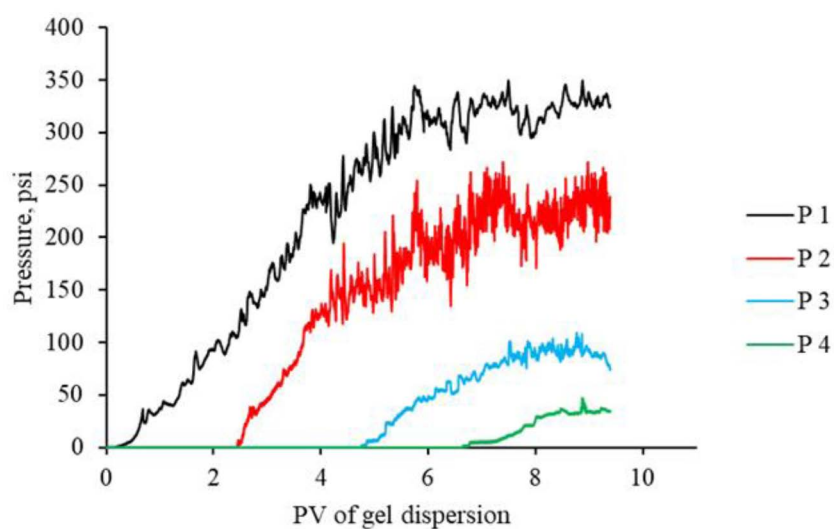

Figure. 6—Injection pressure curve at each pressure sensor across the sandpack, exp 4.

To assess the propagation of micro-RPPG in the sandpack, the pressure gradients in different sections were estimated, as shown in Fig. 7. For experiment 5, the pressure curves in sections 1 and 2 closely overlap, indicating a near-identical propagation of gel particles in these two sections. The minimal deviation between the curves suggests that the gel particles move at a similar rate and experience comparable pressure gradients in both sections. The estimated average injection pressure gradients for sections 1 and 2 are approximately 305 psi/ft and 315 psi/ft, respectively. On the contrary, the injection pressure gradients observed in section 3 and section 4 are notably lower, measuring approximately 131 (psi/ft) and 95 (psi/ft), respectively. These lower values indicate restricted gel propagation within these sections. The acceptable gel injection pressure gradient in oilfields can vary depending on various factors such as reservoir properties, wellbore conditions, and the specific objectives of the operation.
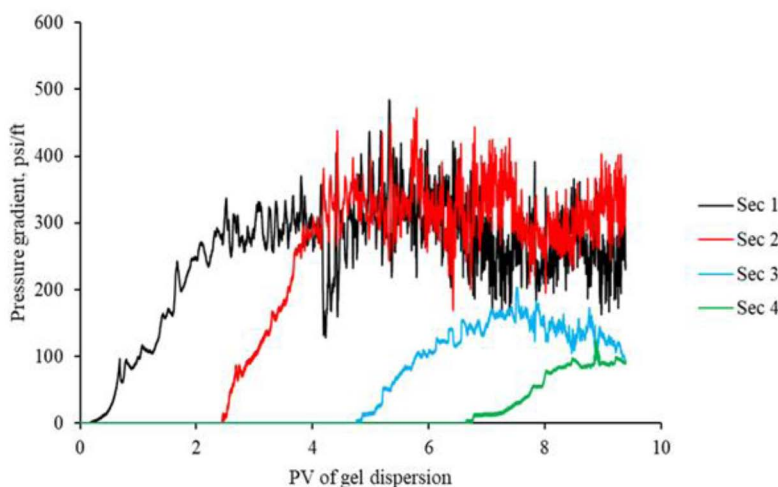
Figure. 7—Injection pressure gradient curve at each sandpack section, exp 4.

Effect of the Gel Concentration and Particle/pore Ratio on Injection Pressure.   Three experiments (Exp 1, 2, and 3) were conducted to study the effect of micro-RPPG concentration on injectivity behavior. In Fig. 8, it can be observed that as the gel concentration increases, the injection pressure gradient also increases. Specifically, for gel concentrations of 3000 and 5000 ppm (average stable pressure at P1 are 190 and 235 psi, respectively), the injection pressure gradients are relatively close. However, the pressure is significantly higher at a gel concentration of 7000 ppm (380 psi). After the micro-RPPG was produced from the outlet, the injection pressure kept increasing in a fluctuating pattern resembling a "zigzag" before eventually stabilizing. Increasing the injection concentration resulted in a greater influx of micro-RPPG entering the sandpack. Consequently, more Micro-RPPG was retained within the model through mechanisms such as "single capturing," "bridging," and "accumulation". Moreover, the compaction degree of the retained micro-RPPG increased proportionally with the concentration of injection.
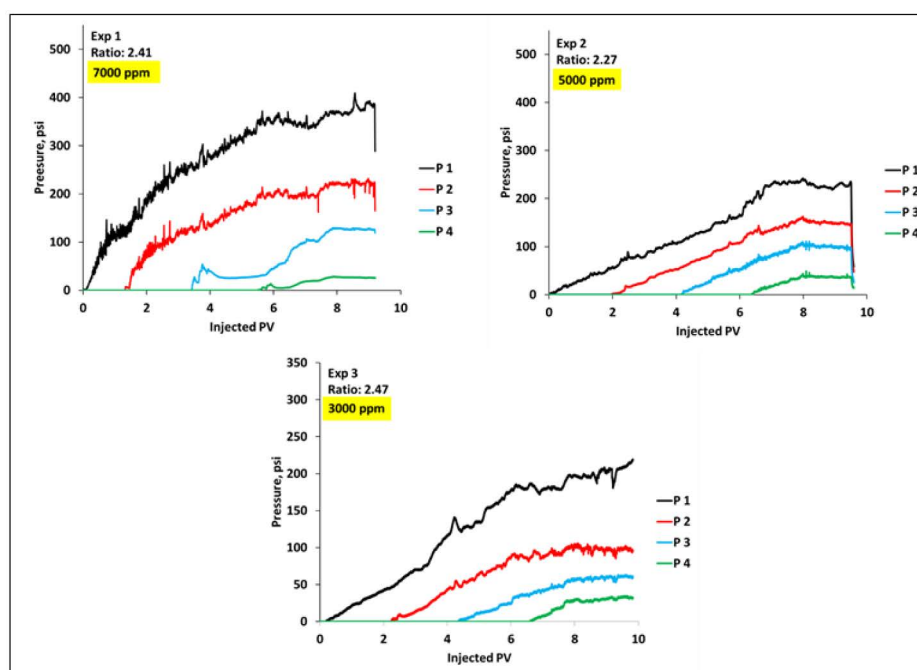

Figure. 8—Effect of the gel concentration on the injection pressure curve.

On the other hand, in Fig. 9, the effect of the particle/pore ratio on micro-RPPG was investigated. In these experiments, the gel concentration was held constant at 5000 ppm. As the particle/pore ratio increases, the stable injection pressure increases. In all six experiments, we observed that the highest stable pressure (485 psi) coincided with the highest particle/pore ratio of 6.05. This observation suggests that increasing the particle/pore ratio results in higher injection pressure during gel placement. Upon entering the sandpack, the particle gel plugged the macropores through single capturing, leading to an elevation in pressure. As the injection pressure reached a specific threshold, the viscoelastic properties caused the gel particle to deform and penetrate deep into the sandpack. Notably, as the particle gel size and strength increased, the pressure required to induce this deformation and subsequent plugging also increased, resulting in higher injection pressure.
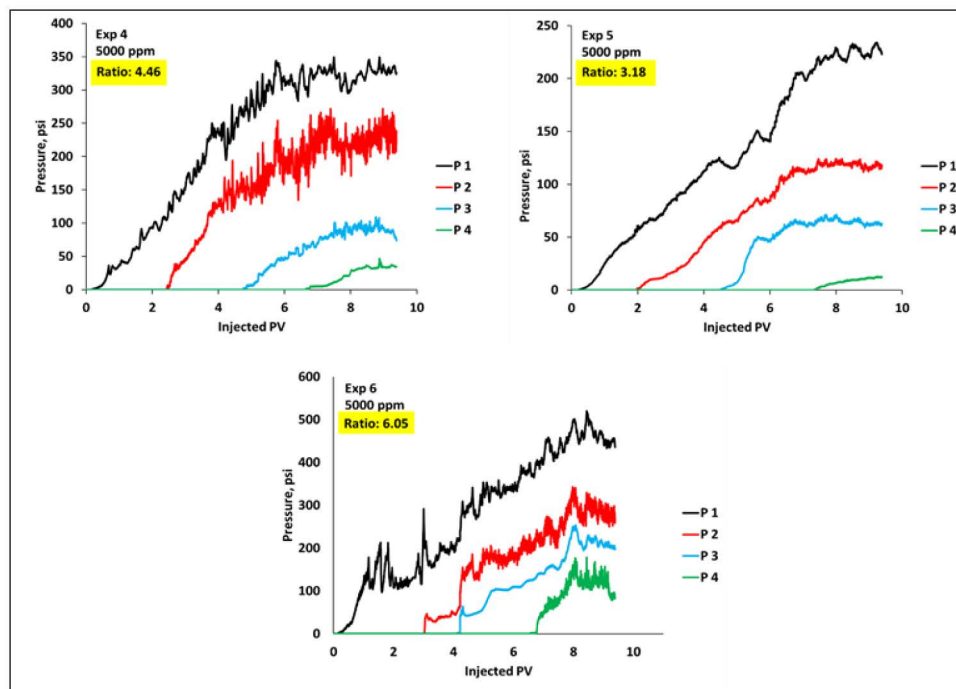

Figure. 9—Effect of the gel particle/pore ratio on the injection pressure curve.

Effect of the Gel Concentration and Particle/pore Ratio on Resistance Factor. The resistance factor (Fr) of the gel (also known as the resistance coefficient) is equal to the ratio of pressure gradient during gel injection to the initial brine injection at the same flow rate. It quantifies the gel's resistance to flow and its ability to maintain its structural integrity. A higher gel resistance factor indicates a stronger and more resilient gel that can effectively plug fractures or block fluid flow. The stable resistance factor for each experiment is summarized in Fig. 10 and 11. At a constant gel concentration of 5000 (ppm), the resistance factor slightly increases with an increase in the particle/pore ratio. The highest value of 3369 was observed for a particle ratio of 6.05. For the same gel concentration, it was observed that the lowest resistance factor value of 1738 was obtained for a suspension gel prepared with formation water, despite the particle/pore ratio not being the lowest in that case. This observation suggests that when formation water was used to prepare the gel suspension, it could form a highly deformable particle gel. This property is desirable for deep particle gel injection and indicates better injectability and potential for effective flow diversion. In contrast, a significant increase in the resistance factor was observed for similar particle/pore ratios (2.47, 2.27, and 2.41) but with different gel concentrations. For gel concentrations of 3000, 5000, and 7000 ppm, the corresponding resistance factor values were 1544, 2128, and 3225, respectively. These results indicate that the gel concentration has a more significant impact on the resistance factor value compared to the

particle/pore ratio. Higher gel concentrations tend to result in higher resistance factors, signifying a greater permeability reduction and impeding fluid flow.
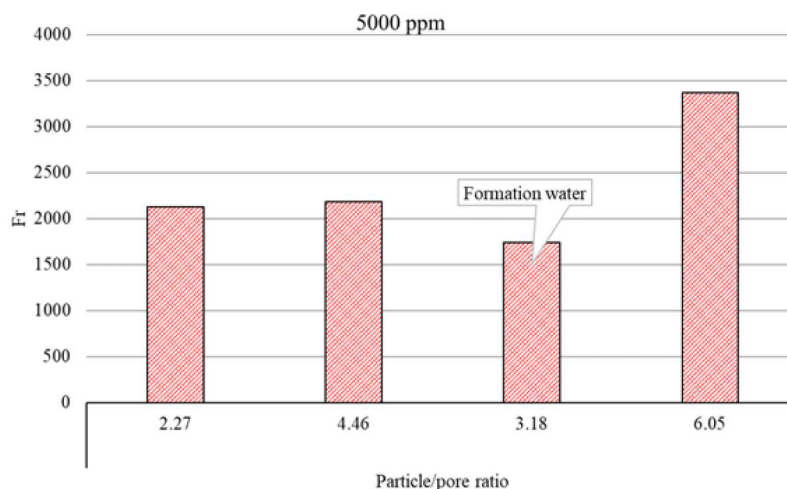
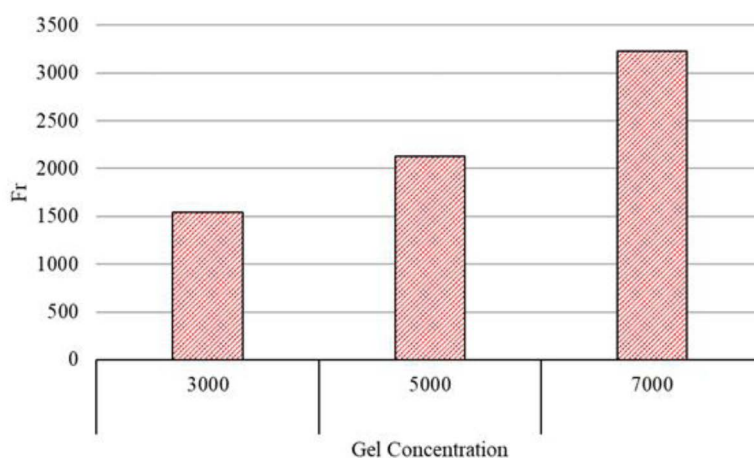**Figure. 10—Effect of the gel particle/pore ratio on F_r at a constant concentration.**

Figure. 11—Effect of the gel particle/pore ratio on F_r at a constant concentration.

Micro-RPPG Retention. During the flow of a micro-RPPG suspension through sandpack, a significant amount of gel particle retention is typically observed. This retention is primarily attributed to the processes of surface adsorption, entrapment, or a combination of both. In this section, the retention (Q, in μg/g) of micro-RPPG in the sandpack system was quantitatively evaluated at various suspension concentrations by using Eq. 8 (Sang., et al 2014).

$$Q = \frac{(c_0 V_0 - \sum c_i V_i)}{M} \tag{7}$$

where C_0 is the concentration of the injected micro-RPPG solution (mg/ L), V_0 is the accumulated injection volume (mL), and C_i is the effluent gel concentration (mg/L). Vi is the effluent volume (mL), and M is the mass of dry sand.

Table. 3 summarizes the calculated retention values for different gel concentrations. The retention of micro-RPPG showed limited increases for concentrations of 3000 and 5000 ppm, whereas a significant increase was observed for a gel concentration of 7000 ppm.

Table 3—Results of micro-RPPG retention in the sandpack.

Exp #	Gel Conc (ppm)	Retention (µg/g)
3	3000	3,860
4	5000	3,985
1	7000	4,260

Micro-RPPG Plugging Performance

After the placement of micro-RPPG in the sandpack, the system was shut off for 72 hrs., allowing the gel to re-crosslink under ambient conditions. Subsequently, the plugging performance was evaluated based on several factors. These included determining the post-brine breakthrough pressure, calculating permeability reduction, and the residual resistance factor.

Post-brine Breakthrough Pressure. Fig. 12 illustrates the post-brine injection pressure as a function of time for Exp 4. The initial permeability of the sandpack was 52 Darcy (D), and after the gel placement, the permeability was reduced to 23 (mD), indicating a significant reduction in permeability. This reduction corresponds to a plugging efficiency of 99.96%. The injection began with a flow rate of 1.5 cc/min. For the pressure sensor P1, as the injection progressed, the pressure steeply increased. However, there was a sudden pressure drop at 125 psi followed by an increase, eventually reaching a peak value. This peak value corresponded to the point at which the brine breakthrough (the pressure at which water begins to produce at the outlet) occurred (at 207 psi), penetrating the re-crosslinked gel and causing a decline in pressure. A stable pressure condition was achieved after the brine was produced in the effluent (average stable pressure is 165 psi). Once the flow rate was increased to 2.0 cc/min, a steep increase in pressure occurred, eventually leading to another peak value at 314 psi, and the average stable pressure was 213 psi. The stable pressure increase was insignificant for flow rates of 2.5 and 3.0 cc/min compared to the flow rates between 1.5, 2.0, and 2.5 cc/min. This suggests that further flow rate increases did not substantially increase the stable pressure beyond a certain flow rate value. The obtained result agrees with the findings of (Imqam et al., 2014). Their study also revealed that preformed particle gel (PPG) injection pressure did not increase linearly with all gel injection flow rates but reached a plateau after a certain injection flow rate.
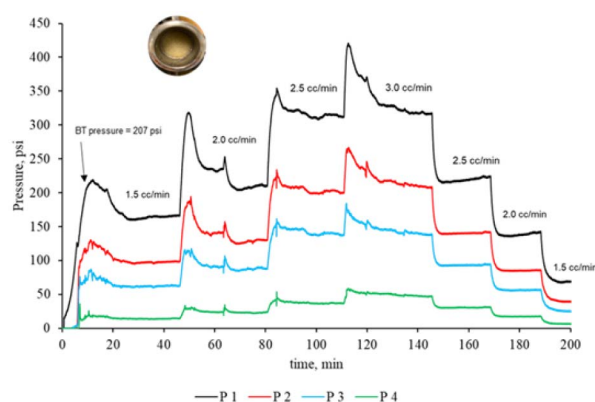

Figure. 12—Post brine injection pressure at each pressure sensor for, Exp 4.

Table. 4 summarizes the breakthrough pressures for each sandpack experiment. The results indicate that the highest breakthrough (298 psi at a flow rate of 1.5 cc/min) pressure corresponds to the experiments with a higher particle/pore ratio. Contrarily, when formation water was used in experiment 5, the lowest breakthrough pressure (111 psi) was observed. This result indicates that the salinity noticeably affects the plugging performance of micro-RPPG. This finding is consistent with the previous bottle tests, which

also demonstrated delays in the re-crosslinking process of micro-RPPG prepared with formation water. Furthermore, the gel strength was found to be lower compared to microgels prepared with 2% KCl.

Table 4—Breakthrough pressure (BT) and plugging efficiency for all experiments.

Exp #	Particle/pore ratio	Suspension Conc.	Brine BT Pressure @ 1.5 cc/min	Plugging efficiency	*F_{rrw}
1	2.41	7000 ppm	237 psi	99.96%	2,811
2	2.27	5000 ppm	186 psi	99.95%	2,093
3	2.47	3000 ppm	147 psi	99.93%	1464
4	2.46	5000 ppm	203 psi	99.96%	2,260
5	3.18	5000 ppm	111 psi	99.93%	1339
6	6.05	5000 ppm	298 psi	99.97%	5948

*F_{rrw}: The calculated value is for the entire sandpack.

Fig. 13 depicts a portion of consolidated sand particles extracted from a sandpack after the completion of the injection process. As shown, Micro-RPPG has exerted a strong consolidating effect on the sand particles, effectively binding them together and giving rise to the observed cohesive structure. This consolidation is attributed to the gel's ability to re-crosslink after being placed into the sandpack. The re-crosslinking process allows the gel to solidify and firmly hold the sand particles together, forming a cohesive matrix and thus improving the plugging efficiency.

Figure. 13—Portion of the sand/gel removed from the sandpack.

Effect of Particle/pore Ratio and Gel Concentration on Plugging Performance. The residual resistance factor (F_{rrw}) is the ratio of the brine permeability before and after gel treatment flows through the sandpack., which is a measurement of the permeability reduction caused by gel. Fig. 14&15 summarize the effect of gel particle/pore ratio and concentration on the (F_{rrw}) in all the experiments. The results indicate that for a proximately equal particle/pore ratio (2.27, 2.47, and 3.18), the F_{rrw} values are distributed relatively uniformly across the sandpack sections, except for a specific particle/pore ratio of 2.41 with a high gel concentration. In this case, there is a noticeable deviation from the uniform distribution. Conversely, for a high particle/pore ratio, it is evident that the highest F_{rr} values are observed in sections 1 and 2. It shows that the residual resistance factor of micro-RPPG is a function of both gel concentration and particle/pore ratio. Furthermore, during the post-brine injection, there was no gel washout was detected. This suggests that the gel retains its integrity and remains in place within the porous media.
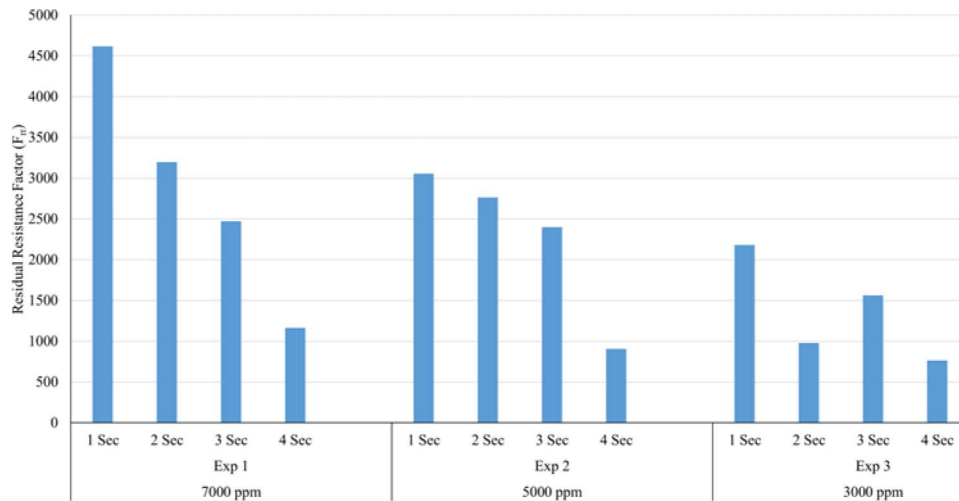
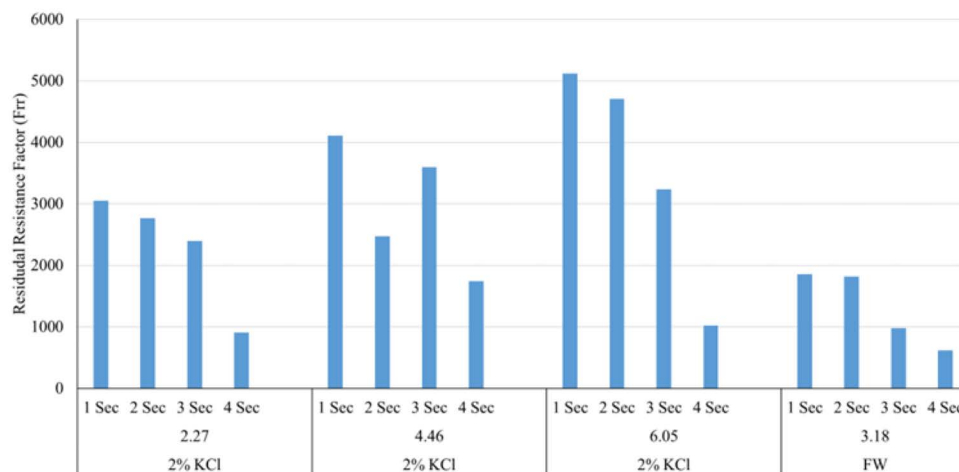**Figure. 14—Effect of the gel concentration on the distribution of F_{rr} in each sandpack section.**

Figure. 15—Effect of the gel particle/pore ratio on the distribution of F_{rr} for a gel concentration of 5000 ppm.

Conclusion

This assessed the feasibility of employing micro-RPPG in field applications, such as hydraulic fractures or porous-medium-type channels. A multi-tape sandpack model with different permeabilities was utilized to simulate relevant conditions and investigate factors affecting the transport behavior of micro-RPPG, including concentration, particle/pore ratio, sandpack permeability, and plugging performance.

- The tested micro-RPPG systems could propagate deeply through the sand pack tube model, which has been demonstrated by the relatively uniform pressure gradient distribution along the sandpack. The gel systems could re-crosslink after being placed in the sandpack.
- The injection pressure of the micro-RPPG increases with particle concentration and particle/pore ratio.
- The post-brine breakthrough pressure for micro-RPPG passing through the sandpack increases as the size ratio of the gel particle to pore and the retention increases.
- The plugging performance results show a substantial reduction in permeabilities, providing a high level of resistance to subsequent waterflooding, with a blocking efficiency of over 99.97%.
- Controlling the injection behavior of micro-RPPG can be achieved by maintaining optimal gel concentration, particle/pore size, and gel strength. These factors play a crucial role in ensuring improved injectivity and overall effectiveness.

- Formation water reduces particle swelling ratio but still can make the particle maintain good plugging efficiency to high permeability channels.

Acknowledgments

References

Bai, B., Liu, Y., Coste, J. P., & Li, L. (2004). Preformed particle gel for conformance control: Transport mechanism through porous media. Proceedings - SPE Symposium on Improved Oil Recovery, 2004-April (January 2004), 17–21. https://doi.org/10.2118/89468-ms

Bai, B., Wei, M., & Liu, Y. (2013). Field and lab experience with a successful preformed particle gel conformance control technology. *SPE Production and Operations Symposium, Proceedings*, 506–522. https://doi.org/10.2118/164511-ms

Chauveteau, G., Omari, A., Tabary, R., Renard, M., & Rose, J. (2002). Controlling gelation time and microgel size for water shutoff. *JPT, Journal of Petroleum Technology*, **53**(3), 51–52. https://doi.org/10.2118/0301-0051-jpt

Coste, J.-P., Liu, Y., Bai, B., LI, Y., Shen, P., Wang, Z., & Zhu, G. (2007). In-Depth Fluid Diversion by Pre-Gelled Particles. *Laboratory Study and Pilot Testing*. https://doi.org/10.2523/59362-ms

Dalrymple, D., Eoff, L., Vasquez, J., & Van Eijden, J. (2008). Shallow penetration particle-gel system for water and gas shutoff applications. Society of Petroleum Engineers - SPE Russian Oil and Gas Technical Conference and Exhibition 2008, **1**, 251–257. https://doi.org/10.2118/114886-ms

Goudarzi, A., Zhang, H., Varavei, A., Taksaudom, P., Hu, Y., Delshad, M., Bai, B., & Sepehrnoori, K. (2015). A laboratory and simulation study of preformed particle gels for water conformance control. *Fuel*, **140**, 502–513. https://doi.org/10.1016/j.fuel.2014.09.081

Gu, F., Wang, W., Cai, Z., Xue, F., Jin, Y., & Zhu, J. Y. (2018). Water retention value for characterizing fibrillation degree of cellulosic fibers at micro and nanometer scales. *Cellulose*, **25**(5), 2861–2871. https://doi.org/10.1007/s10570-018-1765-8

Huh, C., Choi, S. K., & Sharma, M. M. (2005). A rheological model for pH-sensitive ionic polymer solutions for optimal mobility-control applications. SPE Annual Technical Conference Proceedings, 1–13. https://doi.org/10.2523/96914-ms

Imqam, A., Bai, B., Al Ramadan, M., Wei, M., Delshad, M., & Sepehrnoori, K. (2015). Preformed-particle-gel extrusion through open conduits during conformance-control treatments. *SPE Journal*, **20**(5), 1083–1093. https://doi.org/10.2118/169107-PA

Jin, F. Y., Yuan, C. D., Pu, W. F., Zhang, Y. Y., Tang, S., Dong, Y. fan, Zhao, T. hong, & Li, Y. B. (2015). Investigation on gelation process and microstructure for partially hydrolyzed polyacrylic amide (HPAm)–Cr(III) acetate–methanal compound crosslinked weak gel. *Journal of Sol-Gel Science and Technology*, **73**(1), 181–191. https://doi.org/10.1007/s10971-014-3509-z

Larkin, R., & Creel, P. (2008). Methodologies and Solutions to Remediate Inter-Well Communication Problems on the SACROC CO2 EOR Project – A Case Study. https://doi.org/10.2118/113305-ms

Pu, J., Bai, B., Alhuraishawy, A., Schuman, T., Chen, Y., & Sun, X. (2019). A recrosslinkable preformed particle gel for conformance control in heterogeneous reservoirs containing linear-flow features. *SPE Journal*, **24**(4), 1714–1725. https://doi.org/10.2118/191697-PA

Pu, J., Geng, J., & Bai, B. (2018). Effect of the chromium ion diffusion in polyacrylamide/chromium acetate gelation system with surrounding water on gelation behavior. *Journal of Petroleum Science and Engineering*, **171**(August), 1067–1076. https://doi.org/10.1016/j.petrol.2018.08.014

Qiu, Y., Wei, M., & Bai, B. (2017). Descriptive statistical analysis for the PPG field applications in China: Screening guidelines, design considerations, and performances. *Journal of Petroleum Science and Engineering*, **153**(March), 1–11. https://doi.org/10.1016/j.petrol.2017.03.030

Sang, Q., Li, Y., Yu, L., Li, Z., & Dong, M. (2014). Enhanced oil recovery by branched-preformed particle gel injection in parallel-sandpack models. *Fuel*, **136**, 295–306.

Seright, R. S. (1999). Gel treatments for reducing channeling in naturally fractured reservoirs. *SPE Production and Facilities*, **14**(4), 269–276. https://doi.org/10.2118/59095-PA

Smith, D. D., Giraud, M. J., Kemp, C. C., McBee, M., Taitano, J. A., Winfield, M. S., Portwood, J. T., & Everett, D. M. (2006). The successful evolution of Anton Irish conformance efforts. Proceedings - SPE Annual Technical Conference and Exhibition, **6**, 3719–3727. https://doi.org/10.2523/103044-ms

Song, T., Zhai, Z., Liu, J., Eriyagama, Y., Ahdaya, M., Alotibi, A., Wang, Z., Schuman, T., & Bai, B. (2022). Laboratory evaluation of a novel Self-healable polymer gel for CO2 leakage remediation during CO2 storage and CO2 flooding. *Chemical Engineering Journal*, **444**(March), 136635. https://doi.org/10.1016/j.cej.2022.136635

Sydansk, R. D., Al-Dhafeeri, A. M., Xiong, Y., & Seright, R. S. (2004). Polymer gels formulated with a combination of high and low molecular-weight polymers provide improved performance for water-shutoff treatments of fractured production wells. Proceedings - SPE Symposium on Improved Oil Recovery, 2004-April(August), 17–21. https://doi.org/10.2523/89402-ms

Sydansk, R. D., & Southwell, G. P. (2000). More Than 12 Years' Experience With a Successful Conformance-Control Polymer-Gel Technology. *SPE Production & Facilities*, **15**(04), 270–278. https://doi.org/10.2118/66558-PA

Targac, G., Gallo, C., Smith, D., Huang, C. K., Autry, S., Peirce, J., & Baohong, L. (2020). Case history of conformance solutions for west sak wormhole/void space conduit with a new reassembling pre-formed particle gel RPPG. Proceedings - SPE Annual Technical Conference and Exhibition, 2020-Octob. https://doi.org/10.2118/201302-ms

Wu, Q., Ge, J., Ding, L., Wei, K., Deng, X., & Liu, Y. (2021). Identification and characterization of a proper gel system for large-volume conformance control treatments in a fractured tight reservoir: From lab to field. *Journal of Petroleum Science and Engineering*, **198**(July 2020), 108199. https://doi.org/10.1016/j.petrol.2020.108199

Wu, Y. S., & Bai, B. (2008). Modeling particle gel propagation in porous media. Proceedings - SPE Annual Technical Conference and Exhibition, **3**(2007), 1804–1813. https://doi.org/10.2118/115678-ms

Yuan, C., Pu, W., Varfolomeev, M. A., Wei, J., Zhao, S., & Cao, L. N. (2021). Deformable microgel for enhanced oil recovery in high-temperature and ultrahigh-salinity reservoirs: How to design the particle size of microgel to achieve its optimal match with pore throat of porous media. *SPE Journal*, **26**(4), 2053–2067. https://doi.org/10.2118/197804-PA

Zhao, G., You, Q., Tao, J., Gu, C., Aziz, H., Ma, L., & Dai, C. (2018). Preparation and application of a novel phenolic resin dispersed particle gel for in-depth profile control in low permeability reservoirs. *Journal of Petroleum Science and Engineering*, **161**(December 2017), 703–714. https://doi.org/10.1016/j.petrol.2017.11.070